Thermodynamics of Glasses

Jean-Luc Garden, Hervé Guillou

3.2

Thermodynamics of Glasses

Jean-Luc Garden and Hervé Guillou

CNRS, Institut Néel and Université de Grenoble Alpes, Grenoble, France

1 Introduction

Thermodynamics states that the properties of a system in equilibrium depend neither on time nor on past history. Glasses clearly violate this postulate. Not only do their properties depend on history but they also vary with time at temperatures at which relaxation toward internal thermodynamic equilibrium does occur, but at a rate slow enough to be observable at the timescale of the experiment performed. To deal with glasses, thermodynamics must thus consider nonequilibrium states and their actual cause, namely the irreversibility of the transition that occurs when relaxation times eventually become much longer than experimental timescales such that the material freezes in as a glass.

Much attention is currently paid to the processes driving the glass transition at a microscopic scale and also to their implications for the macroscopic properties of glasses. Because this topic is extensively discussed in this chapter, we will deal here with a second fundamental issue, namely that of the phenomenological approaches followed to understand the observable macroscopic properties of glasses and, thus, to design new applications. To quote a single example, density gradients in tempered glasses are the key to thermal strengthening, which is achieved irreversibly upon cooling (Chapter 3.12).

In this chapter, the basic concepts of macroscopic nonequilibrium thermodynamics will first be summarized and illustrated with experimental heat capacities for a model system, PolyVinylAcetate [PVAc, $(C_4H_6O_2)_n$]). The basic concepts of equilibrium and nonequilibrium will then be introduced to point out why glasses challenge the laws of thermodynamics. Next, properties of the supercooled liquid state above T_g will be presented and the phenomenology of the glass transition examined in the light of calorimetric data, in particular in terms of configurational properties. The basics of nonequilibrium thermodynamics in the glass transition range will finally be reviewed along with the issue of aging below the glass transition range.

Reviewers: M.A. Ramos, Laboratorio de Bajas Temperaturas, Universidad Autónoma de Madrid, Spain
A. Saiter, Physics of Materials Group, University of Rouen, Saint-Etienne du Rouvray cedex, France

2 Basics of Nonequilibrium Thermodynamics

In thermodynamics one investigates the changes occurring when a system passes from a state A to another state B. At constant chemical composition, the system is in *internal* equilibrium if its state is defined by only two macroscopic variables such as temperature (T), pressure (P), volume (V), enthalpy (H), internal energy (U), or Gibbs free energy (G). Their values are not only constant but independent of the pathway actually followed between any two states A and B. As stated by the First Law of thermodynamics, between A and B the internal energy varies as:

$$\Delta U_{A\to B} = Q_{A\to B} + W_{A\to B} \quad (1)$$

where $Q_{A\to B}$ and $W_{A\to B}$ are the heat and work exchanged by the system with its surroundings, respectively. Likewise, the entropy is decomposed into two parts,

$$\Delta S_{A\to B} = \frac{Q_{A\to B}}{T} + \Delta_i S_{A\to B}, \quad (2)$$

where the first represents the heat exchanged with the surroundings and the second the entropy created within the system itself during the transformation.

Encyclopedia of Glass Science, Technology, History, and Culture, First Edition. Pascal Richet.

If two equilibrium states are connected by a reversible process, then $\Delta_i S_{A \to B} = 0$. If the system undergoes instead an irreversible process through which it falls out of equilibrium, then $\Delta_i S_{A \to B} > 0$ since a spontaneous process is always associated with an entropy increase of the system. Upon glass formation by cooling, pressure increase, or other means, the equilibrium liquid is continuously losing internal equilibrium. As will be discussed here, the question arises as to whether there is any finite production of entropy and – if so – whether this quantity is of importance regarding the other terms involved in the process.

The Third Law of thermodynamics postulates that the entropy of a perfectly ordered system is zero at 0 K. In contradiction with it, however, calorimetric measurements indicate that glasses not only possess nonzero entropies at 0 K but that this *residual entropy* depends on thermal history as illustrated by a simple entropy cycle calculated from measured heat-capacities and entropy of fusion (ΔS_f). Beginning with a perfectly ordered crystal, whose entropy thus is 0 at 0 K, one derives the entropy of the crystal at its congruent temperature of fusion T_f, then that of the melt from this temperature down to the glass transition, and finally that of the glass down to 0 K (Figure 1). The difference S_0 between this entropy and that of the crystal at 0 K is the residual entropy (Table 2), which increases with higher glass transition temperatures and, thus, with higher cooling rates, reflecting the increasingly wide distribution of configurational states obtaining with increasing temperatures.

A finite residual entropy at 0 K might seem to contradict the Third Law of thermodynamics. As justified by Jones and Simon [1], however, there is no contradiction because this law applies only to crystals and other systems in internal equilibrium, which are necessarily ordered at 0 K to minimize their Gibbs free energies. This is not the case of glasses, which do obey the Nernst theorem [2] since they cannot pass from one entropy state to another at 0 K ($\Delta S = 0$ for two neighboring glassy states at 0 K).

Although such determinations also made for partially disordered crystals like ice I_h or CO have long been explained by simple statistical mechanical models, the very concept of residual entropy has recently been debated [3]. On the assumption that ergodicity must hold for the entropy to be defined, the proponents of a *kinetic* view have claimed that the configurational entropy undergoes an abrupt jump at the glass transition in order to reach the zero value of the crystal entropy at 0 K. In contrast, the proponents of the *conventional* view have stressed that what matters is not time averages but spatial averages of configurational microstates [3], which is the reason why the measured residual entropies do make sense physically and correlate with the specific structural features of glasses and disordered crystals.

By definition, equilibrium thermodynamics cannot alone account for fundamental questions raised when relaxation is too slow with respect to experimental timescales. Owing to the kinetic nature of the problem, use has been made of the formalism originally developed for the kinetics of chemical reactions by De Donder and his school [4]. With values increasing as the reaction proceeds, a new variable, the advancement of reaction, $\xi(t)$ is defined to characterize the state of the system as a function of time, t, such that the reaction rate is simply $d\xi(t)/dt$. This extensive variable, expressed in mol, accounts for the distribution of matter (local mass or density variation), or the molecular structure, within the system at any time. A new state function, the affinity, A, is then introduced to relate $\xi(t)$ to the driving force of the reaction, its Gibbs free energy (at constant T and P):

$$A(P(t), T(t), \xi(t)) = \left(\frac{-\partial G}{\partial \xi}\right)_{P,T} \tag{3}$$

The affinity A, expressed in J/mol, is the intensive conjugate variable of ξ. All time dependences are thus embedded into the time variations of the internal parameter ξ, or A, and of the other variables that are controlled experimentally (e.g. T, P).

For a relaxing system, the instantaneous entropy production was simply written by De Donder as the product of the thermodynamic force and the corresponding flux [4],

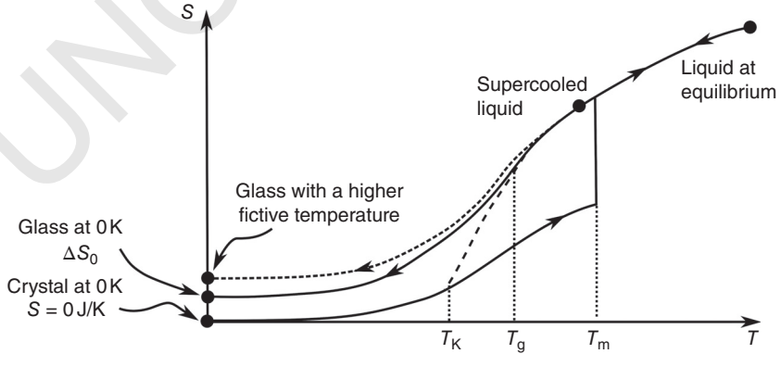

Figure 1 Entropies of the crystal, liquid, supercooled liquid and glass phases of a substance.

Table 1 Thermodynamic states in terms of affinity and its derivatives and in terms of rate of advancement of the process.

Rate of advancement $d\xi/dt$ (extensive, mol/s) Affinity A (intensive, J/mol)	$d\xi/dt = 0$	$d\xi/dt \neq 0$
$A = 0$ and $dA = 0$	True equilibrium; liquid state; $\sigma_i = 0$	Unphysical
$A = 0$ and $dA \neq 0$	Isomassic state; $\sigma_i = 0$	False equilibrium; nonequilibrium state; $\sigma_i = 0$
$A \neq 0$ and $dA = 0$	Isomassic, isoaffine state; $\sigma_i = 0$	Isoaffine state; $\sigma_i \neq 0$
$A \neq 0$ and $dA \neq 0$	Nonequilibrium; glassy state; $\sigma_i = 0$	Nonequilibrium; viscous state; $\sigma_i \neq 0$

Liquid, glass, and relaxing liquid states are indicated by gray cells. The other cells indicate particular states that can be encountered or not during the glass transition. The value of the rate of production of entropy is indicated in each cell.

$$\sigma_i = \frac{\mathrm{d}_i S}{\mathrm{d}t} = \frac{A}{T} \times \frac{\mathrm{d}\xi}{\mathrm{d}t}, \tag{4}$$

where the thermodynamic force actually is A/T, for the sake of dimensional analysis (the entropy production being in W/K).

Regarding the glass transition, the problem boils down to know A and ξ (or $\mathrm{d}\xi/\mathrm{d}t$) and how they evolve with time. Depending on the values of both parameters, however, at this point several cases must be distinguished because not all of them are relevant (Table 1). The first and simplest case is that for which both A and $\mathrm{d}\xi/\mathrm{d}t$ are zero. It is that of the equilibrium liquid, which will thus be first considered in its metastable, supercooled extension.

3 Supercooled Liquids

Although the liquid state is generally far from simple, it can be considered as an equilibrium reference at viscosities (η) low enough that flow is easy, i.e. at high-enough temperatures at the pressure considered. In that case, the diffusion of microscopic entities, be they molecules or atoms, obeys the Stoke–Einstein relation, which relates the diffusivity D to the temperature and viscosity with:

$$D = \frac{k_\mathrm{B} T}{C\eta}, \tag{5}$$

where the coefficient C is a geometrical factor fixed by the boundary condition of the flow.

From its position at time t_0, a diffusing entity travels a kind of random walk over an average distance $d \sim \sqrt{D(t - t_0)}$ as a function of time. For low-viscosity liquids and high temperatures, D is high so that entities explore a great many different positions and configurations in a time shorter than that needed to perform a physical measurement. They do it through degrees of freedom that include not only thermal motions of translation, rotation, and vibration but also the complex kinds of atomic motions collectively termed *configurational*, which are governed by strong short-range repulsions and long-range attractions in molecular liquids. The measurement then averages out all these configurations.

Picturing these motions at a microscopic scale is difficult, however, especially for complex liquids or melts with various interacting entities. In various types of glass-forming liquids [5], local order can nonetheless be described in terms of degree of polymerization, formation of channels or sublattices, or formation of interpenetrating networks. Like the advancement of a chemical reaction, such structural features may be described in terms of the aforementioned parameter ξ. In internal thermodynamic equilibrium, i.e. in the liquid state, ξ is equal to $\xi_\mathrm{eq}(T,P)$, but not in the glass transition range where $\xi(t)$ becomes a function of $T(t)$, $P(t)$, and $A(t)$, revealing its nonequilibrium nature. Below the glass transition range, where the relaxation time of the configurational degrees of freedom exceeds the experimental timescale, they cease to contribute to the measured property. At temperature low enough, the structure then eventually freezes in for good in one state defined by one particular value of $\xi(t)$, which becomes independent of the external parameters T and P.

From a practical standpoint, the timescale defined by the viscosity of the material is important to determine the temperature at which the system will fall out of equilibrium when observed at the timescale of a particular experiment. There is not yet a unique model for describing relaxation phenomena in all glass-forming liquids (Chapter 3.7), whether *strong* or *fragile* with Arrhenian or non-Arrhenian viscosities, respectively [6]. In measurements of macroscopic properties, one nonetheless considers generally that experimental timescales τ_exp are of the order of $\tau_\mathrm{exp} \sim 10^2 - 10^3$ seconds. The viscosity should then be of the order of 10^{12} Pa.s or 10^{13} P for structural relaxation to be complete under these conditions. To stress the usually tremendous variations of viscosity

down to the glass transition, it will suffice to note that the viscosities of stable liquids (i.e. above the melting or liquidus temperature) range from 10^{-3} to 10^{2} Pa.s depending on chemical composition and structural type.

4 Glass as a Nonequilibrium Substance

Time-dependent effects appearing at the glass transition are clearly observed in the heat capacities measured for PVAc (Figure 2), which is a model polymeric system extensively studied because of its excellent glass-forming ability and standard T_g close to room temperature. The observed hysteresis loop between cooling and heating demonstrates that the heat capacity does not only depend on T and P but also on time. Moreover, upon heating, the heat capacity shows a typical overshoot, i.e. an endothermic event, named structural recovery process. To come back to the initial liquid state, the system needs to recover the amount of internal enthalpy that has previously been lost. From such measurements, it is possible to determine the configurational contribution to the heat capacity ΔC_p^{conf}. Here, it is defined by the difference at every temperature between the heat capacities actually measured and estimated for the glass phase:

$$\Delta C_p^{conf} = C_p - C_p^g \tag{6}$$

This type of definition also applies to other thermodynamic variables such as the thermal expansion coefficient α_p, or the isothermal compressibility κ_T. A configurational contribution consequently represents the thermodynamic contribution that originates in configurational changes in the liquid.

The glassy state then is defined as that for which the configurational movements have been frozen-in, i.e. $\Delta C_p^{conf} = 0$. In this state, only the vibrational motions, i.e. the fast degrees of freedom (faster than the experimental timescale), contribute. To define this contribution over the entire temperature interval of interest, an extrapolation of the glass heat capacity from low to high temperatures is needed (Figure 2). The heat capacity of the supercooled liquid can also be extrapolated toward low temperatures (Figure 2). The difference between these values for the supercooled liquid and the glass,

$$\Delta C_p^{conf,eq} = C_p^l - C_p^g \tag{7}$$

then yields the equilibrium configurational contribution, which keeps increasing below T_g even though the actually observed values do vanish (Figure 3).

From the equilibrium and actual configurational contributions, the variation of the configurational enthalpy ΔH^{conf} and entropy ΔS^{conf}, taken between two temperatures, are calculated with:

$$\begin{aligned}\Delta H^{conf}(T) &= \int_{T_1}^{T} \Delta C_p^{conf} dT \text{ and } \Delta S^{conf}(T) \\ &= \int_{T_1}^{T} \frac{\Delta C_P^{conf}}{T} dT\end{aligned} \tag{8}$$

where $T_1 = 360$ K is in Figure 2 an arbitrarily selected reference temperature.

Absolute values of both state functions could be obtained from the enthalpy and entropy of an isochemical crystalline compound through the crystallization values of these functions (see Figure 1). For lack of such a compound for PVAc, only relative values are thus presented (Figure 4) in such a way that both the actual and equilibrium values are equal from 360 K to the temperature of about 315 K at which internal equilibrium is lost. Since these variations are similar for the configurational enthalpy and entropy, only the former is shown in Figure 4.

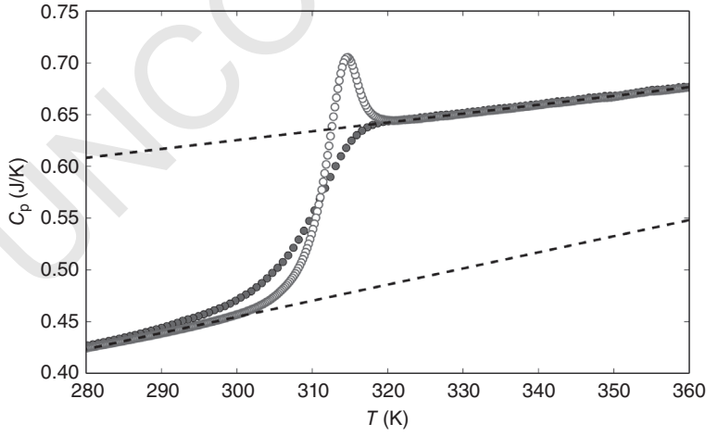

Figure 2 Heat capacity of PVAc measured across the glass transition range by differential scanning calorimetry at the same rate of 1.2 °C/min first upon cooling (solid circle) and then upon heating (empty circle). Dashed lines: fits made from the heat capacities measured for the glass and supercooled liquid.

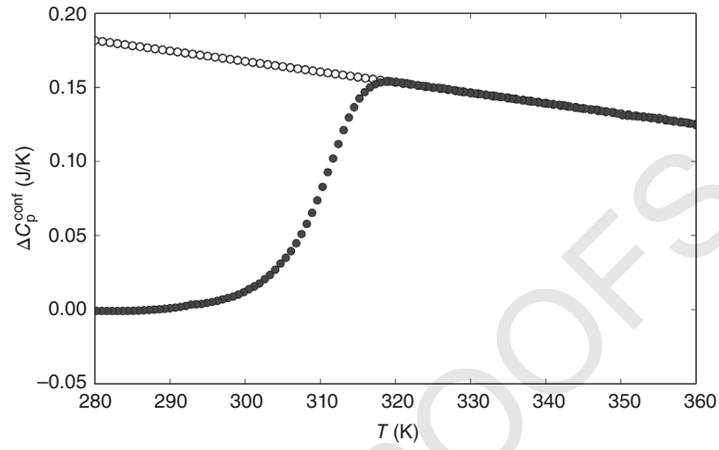

Figure 3 Configurational heat capacity of PVAc across the glass transition range upon cooling: configurational contribution (solid circle) and equilibrium configurational contribution (empty circle).

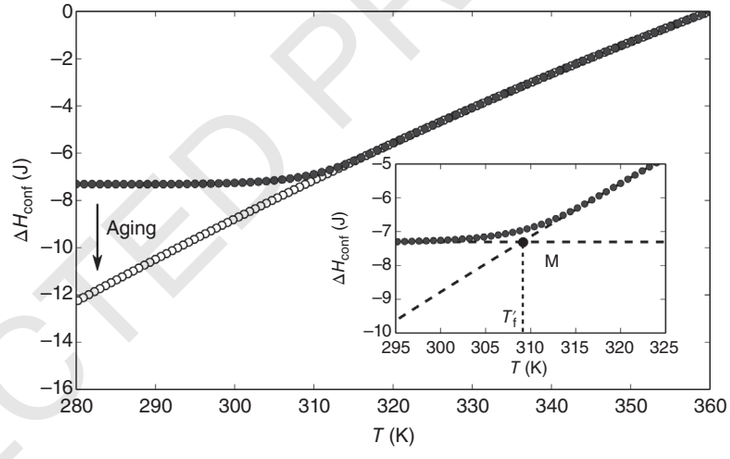

Figure 4 Difference between the configurational enthalpy of PVAc and a zero reference-value taken at 360 K. Actual value (solid circle) and equilibrium value (empty circle). Inset: magnification of Figure 4 showing extrapolated values of the glass and supercooled liquid of this differential configurational enthalpy intersecting at the point *M*, which defines the limiting fictive temperature $T_M = T_f'$.

Contrary to their equilibrium counterparts, which continue to decrease upon cooling, both the actual configurational enthalpy and configurational entropy level off in the amorphous state (Figure 4). Owing to the large width of the glass transition range, the heat capacity variations at the glass transition are much too smooth to be interpreted as reflecting the discontinuity of a second-order phase transition. Such a discontinuity can nonetheless be identified at a temperature T_M defined by the intersection of the extrapolated glass and supercooled liquid (Figure 4, inset). Both configurational enthalpy and entropy are thus continuous at that temperature, which separates the glass from the supercooled liquid. The same applies to other properties such as volume. Because entropy and volume are the first derivatives of the Gibbs free energy with respect to temperature and pressure, respectively, the following relations initially derived by Ehrenfest should hold when second-order derivatives of the free energy vary discontinuously at this point *M*:

$$\left.\frac{dP}{dT}\right|_M = \frac{\Delta\alpha_P}{\Delta\kappa_T} \tag{9a}$$

$$\left.\frac{dP}{dT}\right|_M = \frac{\Delta C_P}{T_M V_M \Delta\alpha_P} \tag{9b}$$

To express these equations in terms of discontinuities of equilibrium configurational contributions at T_M, e.g. $\Delta C_P^{conf,eq}$ of Eq. (7), Prigogine and Defay [7] assumed that the supercooled liquid is in internal equilibrium down to T_M (i.e. $A = 0$ and $dA = 0$) whereas the glass below T_M is defined by $d\xi = 0$. These two equalities can then be grouped to yield the so-called Prigogine–Defay (PD) ratio [7]:

$$\Pi = \frac{\Delta C_P \Delta\kappa_T}{T_M V_M (\Delta\alpha_P)^2} \tag{10}$$

Table 2 Thermodynamic parameters measured from five different glass-formers.

Material	T_g (K)	ΔS_0 (J/K/mol)	PD ratio	T_K (K)	T_0 (K)
SiO_2	1480	5.1	$>10^3$	1150	NA Arrhenius relaxation
$CaAl_2Si_2O_8$	1109	36.2	1.5–22	815	805
Glucose	305	1.7	3.7	241	242
PVAc	301	NA No crystal	2.2	239	250
Glycerol	183	19.4	3.7	134	123
Se	295	3.6	2.4	207	226

The values are taken from the literature.

Although considering an internal parameter ξ, this approach assumes that the glass transition occurs continuously at T_M where $\xi_g = \xi_l$. If so, it would follow from Eq. (9) that the PD ratio should be unity. As indicated by the values listed for widely different glass-forming liquids (Table 2), however, calculated PD ratios are higher or even much higher than unity. One can explain such values by taking into account the kinetic nature of the glass transition [8]. Physically, it is making sense to assume that isobaric temperature derivatives such as ΔC_P or $\Delta\alpha_P$ are not measured under the same kinetic conditions as an isothermal pressure derivative like $\Delta\kappa_T$. Whereas this inconsistency may be removed if more than one internal order parameters ξ are involved in the thermodynamics of the glass transition [9], the problem may in contrast be compounded by the uncertainties arising from the extrapolation procedures used for deriving the relevant parameters at the temperature T_M.

Another puzzling fact has been long ago pointed out by Kauzmann [10] who wondered what would happen if the entropy of a supercooled liquid were extrapolated down to temperatures much lower than the experimentally observed T_g. The conclusion was that it would become lower than that of the isochemical crystal at a temperature T_K, thus termed the Kauzmann temperature (Table 2), which could suggest that the liquid undergoes a continuous phase transition toward the crystalline phase at T_K analogous to the critical point of fluids.

One way out of the paradox implies kinetic arguments and assumes that the viscosity of the supercooled liquid diverges at a temperature close to T_K. This assumption may be represented by the Vogel–Fulcher–Tammann (VFT) equation (Chapter 4.1):

$$\eta = A \exp\left(\frac{B}{T - T_0}\right) \tag{11}$$

where the temperature T_0 of the viscosity divergence is actually close to the Kauzmann temperature (Table 2) even though they may depend on the specific sample and the method of measurement.

Another way out is to take with great caution the extrapolations of the heat capacity and other thermodynamic functions of the supercooled liquid. As long pointed out [e.g. 11], there is no current theory for these properties in liquid state analogous to the Einstein or Debye models that provide functional forms at all temperatures for heat capacities of crystals.

As derived from strikingly old questions in glass science, these counterintuitive features indicate that glasses cannot be described by equilibrium thermodynamic states only. Nonequilibrium thermodynamics is, therefore, likely to be useful to characterize glasses and the glass transition.

5 Nonequilibrium Thermodynamics of the Glass Transition

The questions raised by the Kauzmann paradox or the PD ratio clearly illustrate the need for a more fundamental thermodynamic description of the glass transition. Following the pioneering work of Tool [12, 13] and Davies and Jones [9], different approaches and phenomenological models have been developed to deal with the glass transition range itself, many within the framework of classical nonequilibrium thermodynamics [4, 11].

The starting point has been the phenomenological concept of fictive temperature (T_f) propounded by Tool [12, 13] to characterize the state of a relaxing system at any time. This temperature is similar to an order parameter ξ. It thus overcomes the limitations of the fixed limiting temperature T_M, which characterizes only the point at which internal equilibrium is suddenly lost in a quenched state. On an analogous basis, a more detailed description is made in terms of two-temperature thermodynamics [14] whereby the vibrational and configurational degrees

of freedom are distinguished by a "classical" temperature for fast modes (phonons bath), and an effective temperature for the slow modes, respectively.

The first physical models have then relied on two different approaches. In free-volume theories, one generally considers that the dynamics of the system is determined by the free space present around its atoms, which makes configurational rearrangements more or less easy. In entropy theories, among which that of Adam-Gibbs is the best known [15], the same determining role is attributed to configurational entropy. In other words, these theories assign the strong increase of relaxation times with decreasing temperatures and the eventual structural freezing in to decreases of either free volume or configurational entropy. Other more recent theories of the glass transition rely on mode coupling, random first-order transitions or energy-landscape descriptions [e.g. 16]. These different approaches have the common goal of finding the exact expression for the structural relaxation time, or its distribution, as a function of controlling parameters such as temperature or pressure, or structural order parameter.

For the sake of simplicity, let us consider here conditions of constant pressure. If the additional parameter ξ is taken into account, the total differential of the enthalpy of a system can be written as the sum of two contributions (considering pressure, the generalization to three contributions would be obvious):

$$(\mathrm{d}H)_\mathrm{P} = \left(\frac{\partial H}{\partial T}\right)_{\mathrm{P},\xi} \mathrm{d}T + \left(\frac{\partial H}{\partial \xi}\right)_{\mathrm{P,T}} \mathrm{d}\xi \tag{12}$$

The isobaric heat capacity is written as:

$$C_\mathrm{P} = \left(\frac{\mathrm{d}H}{\mathrm{d}T}\right)_\mathrm{P} = \left(\frac{\partial H}{\partial T}\right)_{\mathrm{P},\xi} + \left(\frac{\partial H}{\partial \xi}\right)_{\mathrm{P,T}} \left(\frac{\mathrm{d}\xi}{\mathrm{d}T}\right)_\mathrm{P} \tag{13}$$

The first term on the right-hand side is the heat capacity at constant ξ, i.e. $C_\mathrm{P}^\mathrm{glass}$, and the second, the configurational contribution $\Delta C_\mathrm{P}^\mathrm{conf}$ as defined by Eq. (6). To account for the kinetic nature of the glass transition, it is then necessary to rewrite Eq. (13) as:

$$C_\mathrm{P} = \left(\frac{\partial H}{\partial T}\right)_{\mathrm{P},\xi} + \left(\frac{\partial H}{\partial \xi}\right)_{\mathrm{P,T}} \left(\frac{\mathrm{d}\xi/\mathrm{d}t}{\mathrm{d}T/\mathrm{d}t}\right)_\mathrm{P} \tag{14}$$

When the rate of change of ξ becomes much smaller than the rate of change of temperature, $(\mathrm{d}\xi/\mathrm{d}t)_\mathrm{P} \ll (\mathrm{d}T/\mathrm{d}t)_\mathrm{P}$, the configurational contribution is negligible.

Hence, it is the ratio between these two rates that is controlling the relative value of the experimentally recorded configurational heat capacity. This ratio is maximum in the supercooled liquid state, and decreases throughout the glass transition range to become negligible in the glassy state (cf. Figure 3). There, only the first right-hand side term in Eq. (14) contributes:

$$\begin{aligned} C_{\mathrm{P},\xi} &= C_\mathrm{P}^\mathrm{glass} < C_\mathrm{P} < C_\mathrm{P}^\mathrm{eq} \\ &= C_\mathrm{P}^\mathrm{liquid} \text{ or } 0 < \Delta C_\mathrm{P}^\mathrm{conf} < \Delta C_\mathrm{P}^\mathrm{conf,eq} \end{aligned} \tag{15}$$

The next step thus consists in taking into account the time dependence of ξ at every temperature through the temperature dependence of the relaxation time τ. The simplest way to do this is to assume a simple exponential decay for ξ at fixed temperature and pressure:

$$\frac{\mathrm{d}\xi}{\mathrm{d}t} = -\frac{\left(\xi - \xi_\mathrm{eq}\right)}{\tau} \tag{16}$$

where $\xi_\mathrm{eq}(P,T)$ is the equilibrium value of the order parameter, i.e. a variable characterizing the liquid structure that depends only on P and T. Although the relaxation time itself has been given different temperature dependences with Arrhenius, VFT, or others laws (Chapter 3.7), the important point is that they are all of an exponential nature with respect to T or P to ensure the structural freezing-in of the system.

Interesting applications of these concepts have been made with the lattice-hole model of liquids, which has the advantage of lending itself to an evaluation of the order parameter ξ. Schematically, this model considers a liquid as a lattice in which disorder is represented by unoccupied sites whose fraction x depends on both temperature and pressure [17]. From the equilibrium value of the order parameter, it is thus possible to solve the linear differential Eq. (16) to find its temperature dependence and, then, to calculate the variations of the heat capacity within the glass transition range under varied conditions [18]. Likewise, the configurational Gibbs free energy may also be computed analytically as a function of temperature, pressure, and order parameter. A similar approach has been followed to incorporate the effects of pressure in the expression of the structural relaxation time for determining also how the heat capacity, thermal expansion coefficient, and isothermal compressibility vary under different conditions [19].

From the configurational Gibbs free energy calculated for the lattice-hole model, one readily simulates with the definition (3) of the affinity its variations upon vitrification (cooling) and structural recovery (heating) [19]. Thermodynamic data measured on *o*-terphenyl may be used to simulate the corresponding affinities during temperature ramps (Figure 5): cooling at 0.3 K/min from an initial temperature of 255 K is followed by heating at the same rate, and then by further cooling at 0.5 K/min preceding final heating at 20 K/min. That the supercooled liquid begins to lose internal equilibrium from 248 K is indicated by the departure at this temperature of the affinity curve from the zero line, which represents the

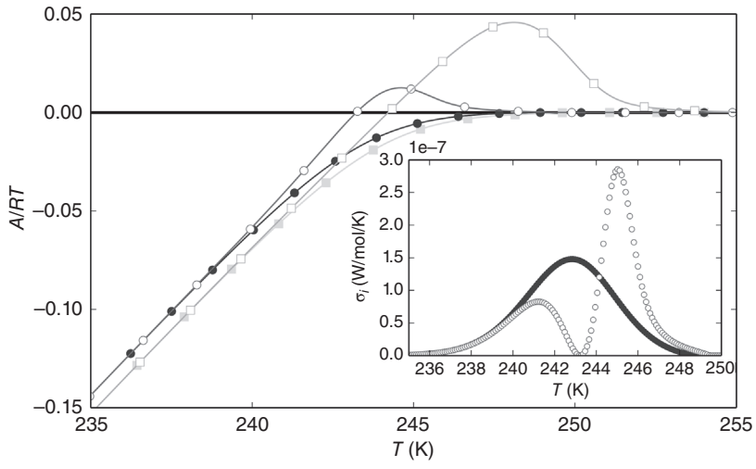

Figure 5 Simulated affinities of *o*-terphenyl in the glass transition range upon cooling and heating as calculated from the lattice-hole model. Solid circle for −0.3 K/min and solid square for −0.5 K/min; empty circle for +0.3 K/min and empty square for +20 K/min. The horizontal line represents equilibrium ($A = 0$). Inset: entropy production rates calculated from the previous affinities. Solid circle upon cooling and empty circle upon heating.

maximum (equilibrium) value of the affinity during cooling. The affinity then linearly decreases with temperature below 240 K in the glassy state, with higher values for slower cooling as a result of lower glass transition temperatures. Upon heating, the affinity begins to increase linearly according to the same line pathway before crossing the equilibrium line. It then exhibits a peak whose position shifts toward higher temperatures and whose magnitude and width increase with the heating rate in ways such that the configurational heat capacity and the other thermodynamic coefficients can be simulated [19].

The entropy production can also be calculated from Eq. (4) (inset in Figure 5). In agreement with previous results [18], it shows a single peak upon cooling but two peaks upon heating. With respect to the experimental data, the advantage of the calculation is thus to distinguish clearly two contributions to the entropy produced when heat is brought to the material. The first peak is associated with a decrease of the configurational energy of the system, which is taking place because of the delay introduced by the relaxation time, even though heat is being supplied. As to the second peak, it is in contrast associated with the configurational energy necessary to recover internal equilibrium in the supercooled liquid state.

Here the wording "is associated" instead of "represents" is necessary because the entropy produced and configurational entropy changes necessarily differ as a result of the irreversible nature of the glass transition. Whereas the entropy production is the product of the thermodynamic force and flux (see Eq. (4)), the variation of the configurational entropy is written as, see Eqs. (8) and (13):

$$\frac{\mathrm{d}S^{\mathrm{conf}}}{\mathrm{d}t} = \frac{\Delta C_{\mathrm{P}}^{\mathrm{conf}}}{T} \times \frac{\mathrm{d}T}{\mathrm{d}t} = \frac{(\partial H/\partial \xi)_{\mathrm{p,T}}(\mathrm{d}\xi/\mathrm{d}t)_{\mathrm{P}}}{T} \quad (17)$$

The rate of entropy production thus reflects the spontaneous or irreversible microscopic processes that take place within the system during relaxation. As dictated by the Second Law of thermodynamics, it is always positive whether upon cooling or heating (Figure 5, inset). Physically, it can be thought of the heat irreversibly generated by friction at a microscopic scale. The resulting thermal power $P_i = T\sigma_i$, where σ_i is the entropy creation in Eq. (4), is produced much too quickly to be compensated instantaneously by an exchange of heat with the surrounding heat bath. Under this circumstance, this is why an effective or fictive temperature can be defined. This surrounding heat bath is sometimes called the phonon bath since it is characterized by fast or vibrational modes.

On the contrary, the change in configurational entropy is a reversible process related to the heat exchanged with the surrounding heat bath whose relevant thermal power is:

$$P_{\mathrm{th}} = T\frac{\mathrm{d}S^{\mathrm{conf}}}{\mathrm{d}t} = \Delta C_{\mathrm{P}}^{\mathrm{conf}} \times \frac{\mathrm{d}T}{\mathrm{d}t}. \quad (18)$$

Because the configurational entropy becomes constant upon vitrification, its variations have vanished (i.e. the configurational heat capacity) below the glass transition range. Above this range, in the supercooled liquid state, they of course differ from zero as indicated by

$$\begin{aligned}\frac{\mathrm{d}S^{\mathrm{conf,eq}}}{\mathrm{d}t} &= \frac{\Delta C_{\mathrm{P}}^{\mathrm{eq}}}{T} \times \frac{\mathrm{d}T}{\mathrm{d}t} \\ &= \frac{(\partial H/\partial \xi)_{\mathrm{P,T}}^{\mathrm{eq}}\left(\mathrm{d}\xi_{\mathrm{eq}}/\mathrm{d}T\right)}{T} \times \frac{\mathrm{d}T}{\mathrm{d}t}\end{aligned} \quad (19)$$

In the transition range, the variations of the configurational entropy of the system are consequently positive or negative upon heating and cooling, respectively. As

already evaluated long ago either theoretically [9] or experimentally [20, 21], the entropy produced is generally negligible with respect to the configurational entropy changes. The integration of the heat capacity curves measured by calorimetry is thus a pertinent way to access to the absolute value of the residual entropy at 0 K [3]. As seen from a direct comparison of Eqs. (4) and (17), arriving at this conclusion is tantamount to neglecting the affinity with respect to the enthalpy of advancement of the configurational change at every temperature:

$$\text{Entropy production negligible} \Longleftrightarrow A \ll \left(\frac{\partial H}{\partial \xi}\right)_{P,T} \tag{20}$$

6 Physical Aging

Relaxation times that depend only on temperature and pressure have been considered. Nevertheless, the complexity of microscopic structures in glasses implies the existence of a distribution of relaxation times. Relaxation processes then also depend on the instantaneous state of the system itself and, thus, on its history as, for instance, described by the Tool–Narayanaswamy–Moynihan model (Chapter 3.7, [22, 23]). A consequence is that some nontrivial relaxation processes can take place well below the glass transition range. Hence, it is interesting to study such a time-dependent process termed *physical aging*, which has a practical relevance through its possible effects on glass properties.

The process can be illustrated with DSC scans for PVAc (Figures 2 and 6). If the sample is cooled down at some rate to 297 K, i.e. about 10 K below the calorimetric T_g, and its temperature is kept constant for a time interval t_a, then its enthalpy (and entropy) relax to their lowest equilibrium values for the temperature (and pressure) considered. Experimentally, physical aging manifests itself as differences between the areas of DSC scans upon heating recorded for samples annealed (72 hours at 297 K) and not annealed. For the experiment without annealing, the lowest temperature of 278 K has been directly reached (see cooling curve in Figure 6). The amount of enthalpy relaxed during aging is equal to the difference between the light gray and dark gray areas in Figure 6. Of course, for a given annealing temperature, such a difference increases with the aging duration. As recently carried out on polymeric glass-formers annealed at relatively low aging temperatures for a very long time, calorimetry (DSC) can bring to light two different timescales for glass equilibration, revealing the complexity and richness of relaxation processes well below T_g [24].

Phenomenologically, however, in simple cases aging can be accounted for with the same approach as developed in previous sections. It is related to the relaxation of the order parameter ξ toward its equilibrium value $\xi_{eq}(P,T)$ whereas the affinity A is relaxing at the same time toward zero. When applicable, the lattice-hole theory can be used to solve Eq. (16) at constant P and T to reproduce the observed process. As done for *o*-terphenyl [19], the order parameter is calculated at constant pressure and aging temperature T = 229.5 K with Eq. (16) and a temperature- and pressure-dependent relaxation time [19]. The affinity has been calculated upon heating at 60 K/min, either after cooling at 6 K/min without aging, or after cooling at the same rate but with an aging process at 229.5 K (Figure 7). Upon isothermal aging, the affinity increases markedly (see the arrow in Figure 6) and then increases at the same rate as without aging. The difference is that the zero line is crossed at a lower temperature so that a much bigger peak is observed when the affinity finally recovers its zero equilibrium value at high temperatures. Since the affinity is an integrated measure of the heat capacity, the large peaks either calculated or

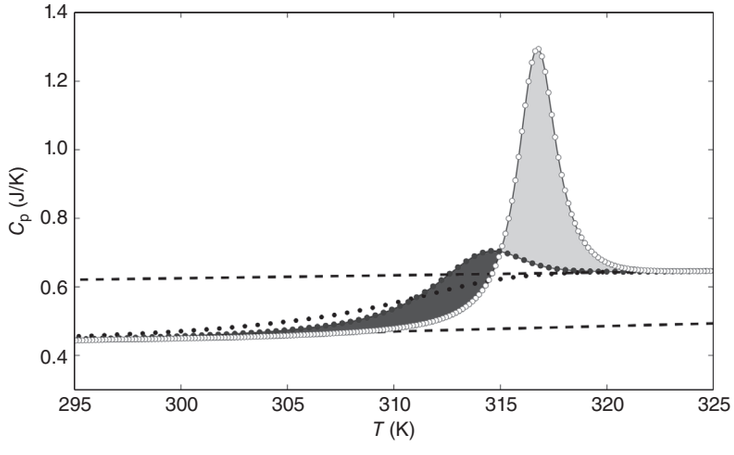

Figure 6 Effect of aging on the heat capacities of PVAc recorded upon heating at the same rate. Heat capacity after a cooling (solid circle with line) and heat capacity after cooling and 72-hour annealing at 297 K (empty circle with line). The enthalpy released during aging estimated by the difference between the two areas included between these two curves. Heat capacities upon continuous cooling shown as solid circles.

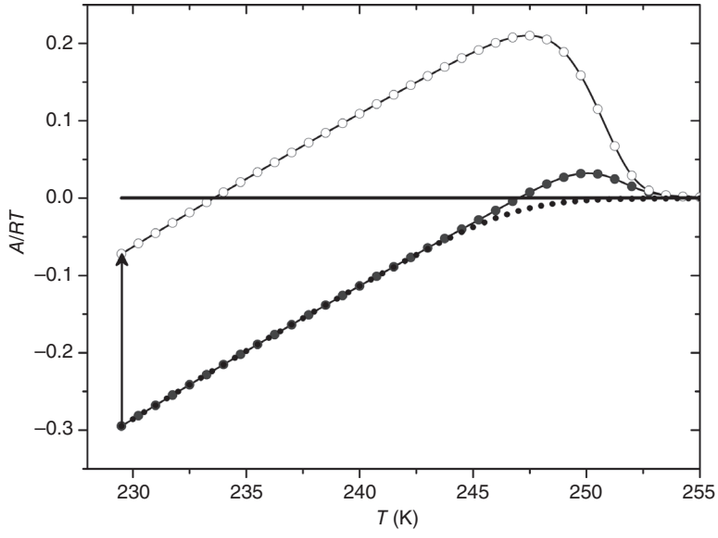

Figure 7 Effect of aging on affinities calculated with the lattice-hole model upon heating at the same rate of 60 K/min, first after a continuous cooling at 6 K/min (black line with solid circle), and second after annealing at 229.5 K (black line with empty circle). The black arrow simulating the relaxation of affinity upon aging at 229.5 K. Affinity upon continuous cooling shown as solid circles.

observed for these properties are clear signatures of aging [19]. More complex calculations can of course be made to deal with at least two separate timescales [24], or a more realistic distribution of relaxation times.

7 Perspectives

Whether in the form of affinity, fictive temperature, or structural order parameter, additional variables must be introduced to deal with the nonequilibrium thermodynamics of glass-forming systems and, in particular, with the time dependence of their properties in relaxation regimes. Phenomenological advances now make it possible to predict these properties as a function of time and temperature or to determine accurately the entropy irreversibly produced, but the mechanisms involved at the atomic or molecular level generally remain to be deciphered. The physical nature of the glass transition is a case in point, as are the origins of Kauzmann catastrophe, of the strong variations of the PD ratio, of the diversity of relaxation timescales or of, as illustrated by the well-known memory effects, the complex nonlinear coupling of the parameters of the differential equations with which these processes are described.

Not only could highly sensitive calorimetric experiments yield valuable original data in this respect but coupling of different techniques such as dielectric spectroscopy and temperature-modulated calorimetry should bring new insights on the dynamics and thermodynamics of the glass transition. Recent experiments on ultra-stable organic glasses obtained by vapor deposition techniques are, for instance, promising [25, 26]. And whereas very long aging performed well below T_g should also give new clues on the laws driving complex relaxation processes in the glassy state [24], experiments made at extremely rapid timescales (e.g. spectroscopy) are in contrast needed to investigate relaxation in supercooled liquids where equilibrium is quickly achieved. To give a single example, ultrastable organic glasses obtained by vacuum-deposition techniques should be of special interest in view of their internal stability that is equivalent of that of hyper-aged glasses (with aging time of millions of years) obtained by conventional melt cooling [25]. For this particular class of glasses, the aforedefined T_M values are so much lower (by a few tens of degrees) than the standard glass transition temperatures that T_M and T_g cannot be indiscriminately used in Eq. (9b) [25, 26]. Among other consequences, new insights should then be gained on the non-unity of the PD ratio. Finally, such experiments should of course be firmly complemented by fundamental work. Microscopic theories and atomistic simulations must be developed and, as stringent tests of their value, their predictions checked in terms of macroscopic physical properties.

Acknowledgments

The authors thank J. Richard for data treatments and simulations carried out with the lattice-hole model, G. McKenna for PVAc samples, and the reviewers for their time, remarks, and useful corrections.

References

1 Jones, G.O. and Simon, F.E. (1949). Qu'est-ce qu'un verre? *Endeavour* 8: 175–181. (in French and in German).
2 Nernst, W. (1969). *The New Heat Theorem*. New York: Dover.
3 Takada, A., Conradt, R., and Richet, P. (2015). *J. Non Cryst. Solids* 429: 33–44.
4 De Donder, T. and Van Rysselberghe, P. (1936). *Thermodynamic Theory of Affinity, A Book of Principles*. Stanford: Stanford University Press.
5 Wondraczek, L., Mauro, J.C., Eckert, J. et al. (2011). Towards ultrastrong glasses. *Adv. Mater.* 23: 4578–4586.
6 Angell, C.A. (1995). Formation of glasses from liquids and biopolymers. *Science* 267: 1924–1935.
7 Prigogine, I. and Defay, R. (1950). *Thermodynamique Chimique, Nouvelle Rédaction*. Liège: Desoer; *Chemical Thermodynamics* (London: Longmans, 1954).
8 Garden, J.-L., Guillou, H., Richard, J., and Wondraczek, L. (2012). Non-equilibrium configurational Prigogine-Defay ratio. *J. Non-Equilib. Thermodyn.* 37: 143–177.
9 Davies, R.O. and Jones, G.O. (1953). Thermodynamic and kinetic properties of glasses. *Adv. Phys. (Phil. Mag. Suppl.)* 2: 370–410.
10 Kauzmann, W. (1948). The nature of the glassy state and the behavior of liquids at low temperature. *Chem. Rev.* 43: 219–256.
11 Nemilov, S.V. (1995). *Thermodynamic and Kinetic Aspects of the Vitreous State*. Boca Raton: CRC Press.
12 Tool, A.Q. (1945). Relaxation of stresses in annealing glass. *J. Res. Natl. Bur. Stand.* 34: 199–211.
13 Tool, A.Q. (1946). Relation between inelastic deformability and thermal expansion of glass in its annealing range. *J. Am. Ceram. Soc.* 29: 240–253.
14 Leuzzi, L. and Nieuwenhuizen, T. (2008). *Thermodynamics of the Glassy State*. New York: Taylor & Francis.
15 Adam, G. and Gibbs, J.H. (1965). On the temperature dependence of cooperative relaxation properties in glass-forming liquids. *J. Chem. Phys.* 43: 139–146.
16 Binder, K. and Kob, W. (2011). *Glassy Materials and Disordered Solids*. Singapore: World Scientific.
17 Simha, R. and Somcynsky, T. (1969). On the statistical thermodynamics of spherical and chain molecule fluids. *Macromolecules* 2: 342–350.
18 Möller, J., Gutzow, I., and Schmelzer, J.W.P. (2006). Freezing-in and production of entropy in vitrification. *J. Chem. Phys.* 125: 094505-1–094505-13.
19 Garden, J.-L., Guillou, H., Richard, J., and Wondraczek, L. (2012). Affinity and its derivatives in the glass transition process. *J. Chem. Phys.* 137: 024505-1–024505-10.
20 Bestul, A.B. and Chang, S.S. (1965). Limits on calorimetric residual entropies of glasses. *J. Chem. Phys.* 43: 4532–4533.
21 Tombari, E. and Johari, G.P. (2014). Change in entropy in thermal hysteresis of liquid-glass-liquid transition and consequences of violating the Clausius theorem. *J. Chem. Phys.* 141: 074502-1–074502-5.
22 Moynihan, C.T., Macedo, P.B., Montrose, C.J. et al. (1976). Structural relaxation in vitreous materials. *Ann. N. Y. Acad. Sci.* 279: 15–35.
23 Narayanaswamy, O.S. (1971). A model of structural relaxation in glass. *J. Am. Ceram. Soc.* 54: 491–498.
24 Cangialosi, D. (2014). Dynamics and thermodynamics of polymer glasses. *J. Phys. Condens. Matter* 26: 153101-1–153101-19.
25 Swallen, S.F., Kearns, K.L., Mapes, M.K. et al. (2007). Organic glasses with exceptional thermodynamic and kinetic stability. *Science* 315: 353–356.
26 Rodríguez-Tinoco, C., González-Silveira, M., Barrio, M. et al. (2016). Ultrastable glasses portray similar behaviour to ordinary glasses at high pressure. *Sci. Rep.* 6: 34296–1–10.